

# Ground based gamma-ray astronomy with Cherenkov Telescopes

**Jim Hinton**

School of Physics & Astronomy, University of Leeds, Leeds LS2 9JT, UK

E-mail: [j.a.hinton@leeds.ac.uk](mailto:j.a.hinton@leeds.ac.uk)

**Abstract.**

Very-high-energy ( $>100$  GeV)  $\gamma$ -ray astronomy is emerging as an important discipline in both high energy astrophysics and astro-particle physics. This field is currently dominated by Imaging Atmospheric-Cherenkov Telescopes (IACTs) and arrays of these telescopes. Such arrays have achieved the best angular resolution and energy flux sensitivity in the  $\gamma$ -ray domain and are still far from the fundamental limits of the technique. Here I will summarise some key aspects of this technique and go on to review the current status of the major instruments and to highlight selected recent results.

## 1. Introduction

Ground-based  $\gamma$ -ray astronomy effectively began in 1989, with the first detection of a TeV  $\gamma$ -ray source, the Crab Nebula, with the 10 m Cherenkov telescope of the Whipple Observatory [1]. Eighteen years on, Cherenkov telescopes have been used to detect 68 very high energy (VHE;  $E > 100$  GeV) sources, firmly establishing a new astronomical domain. The key advantage of ground based instrumentation over satellite-based GeV instruments such as EGRET and the upcoming GLAST large area telescope (LAT) is collection area. The typical effective collection area of single Cherenkov telescope is  $10^5$  m<sup>2</sup>, almost five orders of magnitude larger than can realistically be achieved via direct detection in space. The major advantage of the Imaging Atmospheric-Cherenkov Telescope (IACT) technique with respect to other ground-based approaches (which are described elsewhere in this volume) is the precision with which the properties of the primary  $\gamma$ -ray can be reconstructed. The angular resolution achievable is currently limited only by the number of Cherenkov photons collected, with the theoretical limit close to  $30''$  at 1 TeV, an order of magnitude better than current instruments have achieved [2]. Indeed, the typical angular resolution of  $0.1^\circ$ , whilst not impressive in comparison to that achieved over much of the electromagnetic spectrum, is the best at any energy above  $\sim 0.1$  MeV.

Here I will summarise the Cherenkov Telescope technique and then summarise the results produced using these instruments.

## 2. The Imaging Atmospheric-Cherenkov Technique

### 2.1. Cherenkov light from air-Showers

High energy ( $> 100$  GeV) photons entering the Earth's atmosphere initiate electromagnetic cascades, via the processes of electron pair-production and subsequent bremsstrahlung. The number of electrons at the point of maximum development of the cascade is closely proportional to the primary energy and the atmospheric depth of this maximum increases logarithmically with energy. For a 1 TeV photon-initiated air-Shower this maximum occurs at a depth of  $\sim 300$  g cm<sup>-2</sup>, or at  $\sim 10$  km above sea level (a.s.l.) for a vertically incident photon. Electrons and positrons in the shower with energies greater than  $m_e c^2 / \sqrt{1 - n^{-2}}$  will emit Cherenkov light. This threshold corresponds to  $\approx 20$  MeV in air at sea level and roughly twice that at 10 km a.s.l. The yield of Cherenkov light is proportional to the total track length of all particles (in the ultra-relativistic limit) which is in turn proportional to the primary energy. In this way an image of the cascade in Cherenkov light provides a pseudo-calorimetric measurement of the shower energy. The opening angle of Cherenkov light in air is roughly  $1^\circ$  and hence the photons produced around shower maximum arrive at typical observation heights of  $\sim 2000$  m a.s.l. in a 'light-pool' of  $\sim 120$  m radius. As can be seen from figure 1, the density of photons within this light pool is roughly 100 photons (of wavelength 300–600 nm) per square-metre per TeV of primary energy. For a typical instrumental efficiency of 10% (reflectivity of mirror

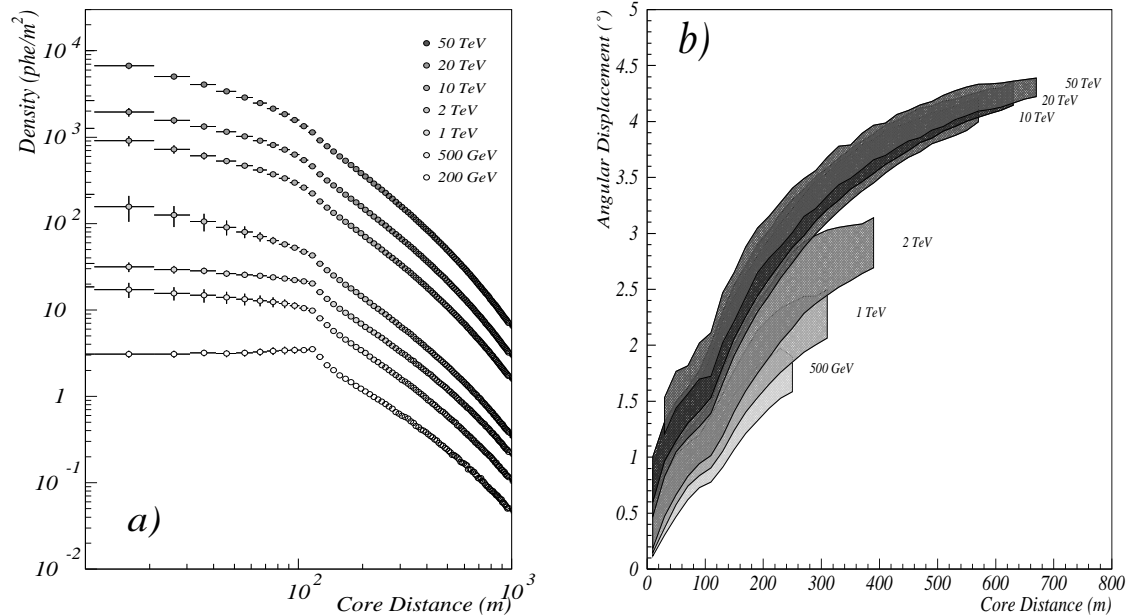


**Figure 1.** a) The lateral distribution of Cherenkov light for  $\gamma$ -ray primaries of various energies at 2400 m altitude. b) The displacement of the centroid of the Cherenkov image as a function of impact distance. Both plots are reproduced from [7].

surfaces; quantum efficiency of photo-sensors), primary reflectors of  $\sim 100 \text{ m}^2$  area are required to produce images containing 100 photoelectrons for 100 GeV  $\gamma$ -ray showers. The fall-off in density outside this region is rather rapid, but as figure 1 illustrates, at very high energies ( $> 10 \text{ TeV}$ ), distant showers (with impact distances of several hundred metres) are visible even with modest sized telescopes. The ‘flash’ of Cherenkov light at the ground lasts only a few nanoseconds. Fast photo-sensors and electronics are therefore employed to resolve the faint Cherenkov signal against the night sky background (NSB) light, which has a typical rate of  $1 \text{ photon-electron} \times (\Delta t/10\text{ns})(\theta/0.1^\circ)^2 (\text{A}/100\text{m}^2)$ . Outside periods of astronomical darkness the background light level is much higher, imposing a  $\sim 10\%$  duty cycle on IACT observations (at least for low energy threshold measurements, see [3]).

As most Cherenkov light from TeV showers is produced around the point of maximum development of the shower, the intensity of light at ground level scales approximately as  $1/d^2$  where  $d$  is the distance to the point of shower maximum, and conversely the area covered by the Cherenkov light pool is proportional to  $d^2$ . Observations at lower altitudes or equivalently greater zenith angles can be used to increase collection area, at the expense of a higher energy threshold (e.g. [4, 5]). Conversely, very high altitude observatories have been suggested as a natural way to achieve lower energy thresholds (e.g. [6]).

Images of  $\gamma$ -ray showers have typical rms widths and lengths of  $\sim 0.1^\circ$  and  $\sim 0.3^\circ$ ,

respectively (at  $\sim 1$  TeV, 100 m impact distance). Pixelisation of not much greater than  $0.1^\circ$  is therefore required to resolve the showers. The displacement of the shower image centroid is directly related to the impact distance of the shower axis with respect to the telescope (see figure 1b). At high energies, the effective collection area for a Cherenkov telescope is therefore often limited by the size of the field of view (FoV), rather than by mirror area (or equivalently photon density). Figure 1b demonstrates that a FoV of at least  $\sim 4^\circ$  is desirable for TeV observations. In fact it is difficult to provide a field of view much bigger than this and maintain an optical point-spread-function (PSF) on the scale of  $<1$  pixel, without the use of secondary optics and hence additional cost and complexity. Cost has also so far limited the total pixel number to less than  $\sim 1000$ , again with implications for the field of view achievable.

## 2.2. $\gamma$ /Hadron separation

As discussed above a rather simple light collector of area  $100 \text{ m}^2$  is sufficient to detect  $\sim 100$  GeV  $\gamma$ -ray showers if placed at mountain altitudes. The major challenge of the Cherenkov technique is the presence of an, at one time, overwhelming background of air-showers initiated by cosmic ray protons and nuclei. For example, for observations with the H.E.S.S. telescope array, the rate of detected photons from the brightest steady sources is still only  $\sim 0.1\%$  of the rate of background showers. Fortunately, showers initiated by TeV protons and nuclei differ in many respects from  $\gamma$ -ray showers. Much of the energy in the primary is transferred to pions produced in the first few interactions. The neutral pions decay to produce electromagnetic *sub-showers*, with the charged pions decaying to produce muons. Single muons reaching ground level produce ring images if impacting the telescope dish, or arcs at larger impact distances. The sub-showers often result in substructure in images and the larger transverse angular momentum in hadronic interactions leads to showers that are generally wider than those of  $\gamma$ -rays. For a given primary energy, hadronic showers also produce less Cherenkov light (a factor  $\sim 2$ – $3$  at TeV energies), due to the energy channelled into neutrinos and into high energy muons and hadrons in the shower core.

The primary discriminator between hadron and  $\gamma$ -ray initiated showers is therefore the width of the Cherenkov image. The breakthrough in the technique was the recognition by Hillas in the 1980's that the measurement and simple parameterisation of images allows very effective background rejection [8, 9]. Several more sophisticated background rejection and shower reconstruction methods have now been developed (see for example [10], [11], [12]) but the ‘‘Hillas parameter’’ approach remains the standard in the field.

Despite the rejection of the vast majority of the background using image cuts, the correct modelling and subtraction of the remaining background is a major challenge and a potential source of systematic errors, see [13] for a recent summary.

### 2.3. Stereoscopic Measurements

The desirability of multiple telescope observations of individual air-showers was first demonstrated by the HEGRA collaboration [14]. The first advantage occurs at the trigger level: an array with a multi-telescope trigger system removes the vast majority of single muons and also many hadron initiated showers. For a dead-time limited system this may allow a lower trigger (and hence energy) threshold, see for example [15]. Other advantages arise at the analysis stage, primarily in the reconstruction of the shower geometry and hence in the reconstruction of the direction and energy of the primary  $\gamma$ -ray. Shower axis reconstruction with a single Cherenkov telescope is possible using the length of the image to estimate the angular distance to the source position [16]. However, the multiple views of the shower provided by stereoscopic observations allow a more accurate determination of the shower direction using the intersection of the directions defined by the major axes of the images recorded in each camera. In a similar way, the shower core location can be better established, leading to improved energy resolution (due the dependence of Cherenkov light intensity on impact distance, see figure 1). The improved shower geometry also leads to better hadron rejection, the primary rejection parameter *width* can be replaced by *mean scaled width*, normalising based on expectations for  $\gamma$ -ray showers (for a given image amplitude and impact distance) and averaged over all telescopes (see for example [17]). The optimal separation of telescopes in an array seems to be close to the radius of the Cherenkov light-pool ( $\sim 100$  m), with closer spacing improving low-energy performance at the expense of effective collection area at higher energies (and vice versa).

### 2.4. The use of timing information

The arrival time structure of Cherenkov images provides a potential additional discriminator against the hadronic background. Single muons certainly exhibit a characteristic very fast time profile [18] and timing information may be useful in rejecting hadronic showers (see for example [19]). Several instruments of the current generation record digitised waveforms and there is evidence to suggest that a significant improvement in background rejection, and hence sensitivity, can be achieved using this information — at least for single telescopes [20]. However, these studies are still at a relatively early stage and it is not yet clear if substantial gains are possible for stereoscopic systems.

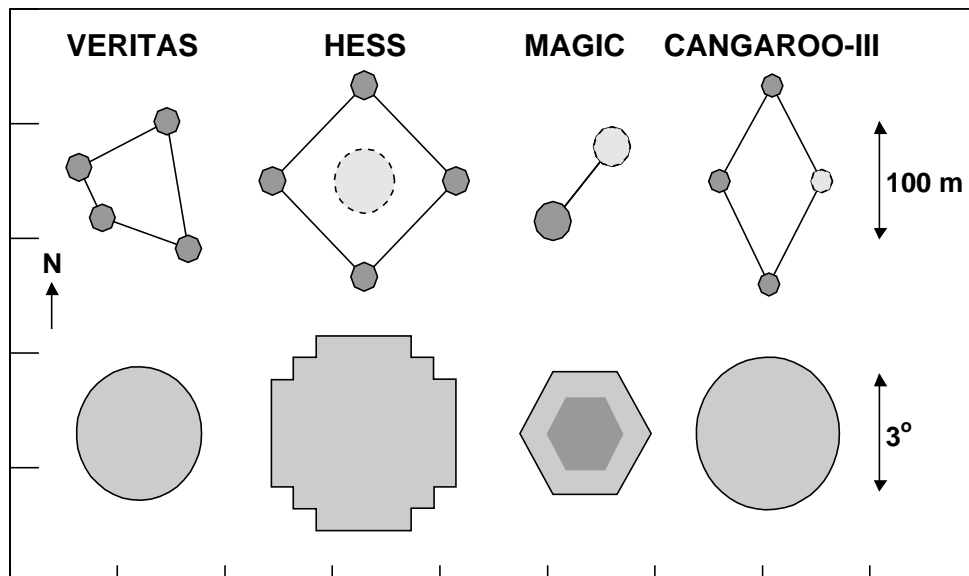
## 3. Current Instruments

Table 1 summarises the characteristics of currently operating Imaging Cherenkov telescopes and arrays, together with some important decommissioned systems. In the following I will discuss the current systems, with emphasis on the major Cherenkov telescope systems illustrated in Figure 2.

*The High Energy Stereoscopic System* (H.E.S.S.) is an array of 4 Cherenkov

**Table 1.** Principle characteristics of currently operating (and selected historical) IACTs and IACT arrays. The energy threshold given is the approximate trigger-level (rather than post-analysis) threshold for observations close to zenith. The approximate sensitivity is expressed as the minimum flux (as a percentage of that of the Crab Nebula:  $\approx 2 \times 10^{-11}$  photons  $\text{cm}^{-2} \text{s}^{-1}$  above 1 TeV) of a point-like source detectable at the  $5\sigma$  significance level in a 50 hour observation. In the cases where this number has not been provided by experimental collaborations, it is estimated here from published detections. \* No refereed publications from this instrument exist and it's sensitivity is therefore very difficult to estimate. † These instruments have pixels of two different sizes.

Instrument	Lat. (°)	Long. (°)	Alt. (m)	Tels.	Tel. Area (m <sup>2</sup> )	Total A. (m <sup>2</sup> )	Pixels	FoV (°)	Thresh. (TeV)	Sensitivity (% Crab)
H.E.S.S.	-23	16	1800	4	107	428	960	5	0.1	0.7
VERITAS	32	-111	1275	4	106	424	499	3.5	0.1	1
MAGIC	29	18	2225	1	234	234	574	3.5 <sup>†</sup>	0.06	2
CANGAROO-III	-31	137	160	3	57.3	172	427	4	0.4	15
Whipple	32	-111	2300	1	75	75	379	2.3	0.3	15
Shalun	43	77	3338	1	11.2	11.2	144	8	0.8	*
TACTIC	25	78	1300	1	9.5	9.5	349	3.4	1.2	70
<i>HEGRA</i>	29	18	2200	5	8.5	43	271	4.3	0.5	5
<i>CAT</i>	42	2	1650	1	17.8	17.8	600	4.8 <sup>†</sup>	0.25	15



**Figure 2.** Comparison of the array layout (top) and camera field of view (bottom) for the major atmospheric Cherenkov detectors. The radius of the circles representing the telescope dishes has been doubled for clarity. The dashed circles indicate telescopes currently under construction. The darker region at the centre of the MAGIC camera illustrates the region with smaller pixel size.

telescopes situated in the Khomas highlands of Namibia [21]. Completed in early 2004, H.E.S.S. was the first of the new generation of Cherenkov Telescope arrays to become fully operational. The H.E.S.S. telescopes have 13 m diameter ( $107 \text{ m}^2$ ) dishes and a focal length of 15 m [22]. The Davis-Cotton optical design allows a wide field with reasonable off-axis optical PSF. The optical PSF has an 80% containment radius of  $1.4'$  on-axis, with the diameter becoming comparable to the camera pixel size ( $0.16^\circ$ ) only at the edge of the field-of-view. The cameras consist of 960 photomultiplier tube pixels, with signal acquisition via 1 GHz analogue ring samplers (ARSs), in normal operation however only the 16 ns integrated signal is read out to reduce dead-time. H.E.S.S. utilises an array level trigger which for normal operations requires a telescope multiplicity of two [15]. Construction has just begun on an upgrade to H.E.S.S. consisting of a single very large ( $600 \text{ m}^2$ ) parabolic telescope at the centre of the phase-1 array [23]

*The MAGIC telescope* on La Palma, in the Canary Islands, is, at 17 m diameter, the largest single Cherenkov telescope in operation and also reaches the lowest trigger-level energy threshold (at  $\approx 60 \text{ GeV}$ ) [24]. The design of the instrument was driven by two goals, to be able to rapidly slew the telescope at respond to  $\gamma$ -ray burst (GRB) alerts, and to achieve an energy threshold as low as possible given the size of the dish. The light-weight construction allows a slewing speed of  $\sim 5^\circ/\text{s}$  ( $\sim 3$  times faster than the H.E.S.S. telescopes) [25]. A parabolic dish removes the time dispersion due to optical path length differences and a recent upgrade to 2 GHz waveform sampling allows exploitation of the timing information in the Cherenkov front (see above). The advantages of a stereoscopic system (as discussed above) motivated the second phase of the MAGIC project: the construction of a second 17 m telescope 85 m from the first. This second telescope is currently under construction and will have a camera with uniform pixel size and an increased trigger region [26].

*VERITAS* (The Very Energetic Radiation Imaging Telescope Array System) is an array of four 12 m diameter telescopes situated at the base-camp of the Whipple Observatory in Arizona [27, 28]. First light for the full four telescope array occurred early in 2007. The overall design, and hence the sensitivity, of the array is rather similar to that of H.E.S.S. [29]. VERITAS has the advantage of 500 MHz flash ADCs, but a somewhat narrower field-of-view, which may limit performance at high energies.

The *CANGAROO-III* instrument [30] is a four telescope system continuing the CANGAROO project [31, 32] on a site near Woomera, Australia. The array of 3 new 10 m diameter telescopes was completed in 2004. A fourth telescope, that of the CANGAROO-II instrument is currently not included in the array trigger, pending a camera upgrade. Some controversy surrounded some detections using CANGAROO and CANGAROO-II, but all disagreements with results from the H.E.S.S. array have now been resolved by observations with the more sensitive CANGAROO-III instrument [33].

Other currently operating Cherenkov instruments include the TACTIC imaging telescope [34] and the non-imaging PACT system (see e.g. [35]), both located in India. PACT is to my knowledge the only remaining non-imaging Cherenkov detector. In the recent past, several converted solar power stations were used to make Cherenkov

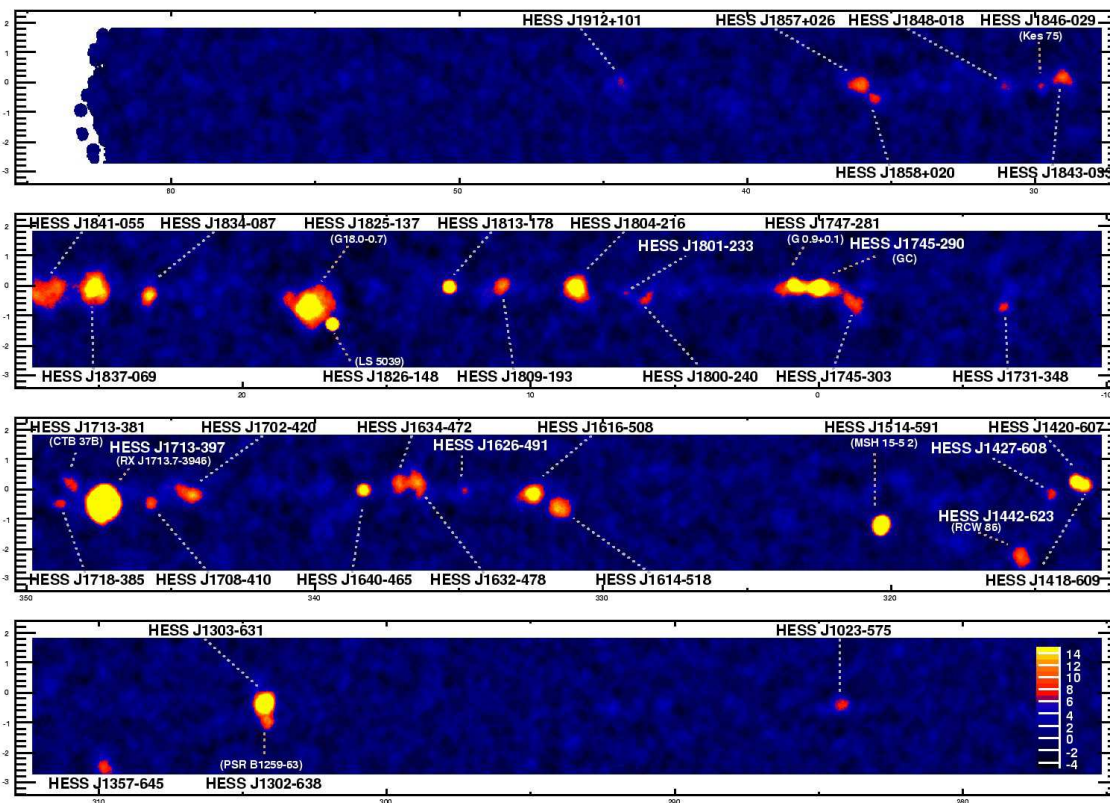


**Figure 3.** The H.E.S.S. survey of the inner galaxy in  $\sim 1$  TeV  $\gamma$ -rays. The colour scale shows the statistical significance for an excess within an  $0.22^\circ$  radius at each position. Image courtesy of the H.E.S.S. Collaboration.

observations at rather low energies (50–150 GeV thresholds) but with modest hadron rejection power and hence sensitivity. These instruments were operated by the CELESTE [36], STACEE [37], Solar Two (later CACTUS) [38], and GRAAL [39] collaborations.

## 4. Recent Science Highlights

### 4.1. Galactic Sources

The recent one order of magnitude growth in the number of known *galactic* VHE  $\gamma$ -ray sources is largely a consequence of the survey of the galactic plane conducted by the H.E.S.S. collaboration between 2004 and 2007 [40, 41, 42]. Figure 3 shows the current extent of this scan, which now covers essentially the whole inner galaxy:  $-85^\circ < l < 60^\circ$ ,  $-2.5^\circ < b < 2.5^\circ$  [42]. Most of the 52 currently known galactic TeV sources remain unidentified. This is in part due to the difficulty of identifying extended sources with no clear sub-structure. Nonetheless, several methods of identification have been successfully applied and the situation is much more favourable than that in the GeV band where only one galactic source class (pulsars) has been unambiguously identified.



**Table 2.** Galactic very high energy  $\gamma$ -ray sources with well established multi-wavelength counterparts. The instrument used to discover the VHE emission is given together with the year of discovery. Fluxes are approximate, and expressed as a percentage of the flux from the Crab Nebula in the TeV range, \* indicates variable emission. The photon index  $\Gamma$  ( $dN/dE \propto E^{-\Gamma}$ ) is given together with its statistical error, systematic errors are typically  $\sim 0.2$ . The final column gives citations to the respective discovery paper and other papers marking significant steps towards the identification of the source. These associations were established through a range of methods, which are given in the table in abbreviated form: *Pos*: The position of the centroid of the VHE emission can be established with sufficient precision that there is no ambiguity as to the low energy counterpart. In practise this is usually only possible for point-like sources. *Mor*: There is a match between the  $\gamma$ -ray morphology and that seen at other (usually X-ray) wavelengths. This requires sources extended well beyond the typical angular resolution of IACTs ( $\sim 0.1^\circ$ ). *EDMor*: Energy-dependent morphology which approaches the position/morphology seen at other wavelengths at some limit, and is consistent with our physical understanding of the source. *Var*:  $\gamma$ -ray variability correlated with that in other wavebands. *Per*: periodicity in the  $\gamma$ -ray emission matching that seen at other wavelengths. Note that all these objects are X-ray sources.

Object	Discovered	Year	Type	Method	Flux	Index	Ref.
PSR B1259–63	HESS	2005	Binary	Pos/Var	7*	$2.7 \pm 0.2$	[43]
LS 5039	HESS	2005	Binary	Pos/Per	3*	$2.12 \pm 0.15^*$	[44, 45]
LSI+61 303	MAGIC	2006	Binary	Pos/Var	16*	$2.6 \pm 0.2$	[46, 47]
RX J1713.7–3946	CANGAROO	2000	SNR Shell	Mor	66	$2.04 \pm 0.04^\dagger$	[48, 49, 50]
Vela Junior	CANGAROO	2005	SNR Shell	Mor	100	$2.24 \pm 0.04$	[51, 52, 53]
RCW 86	HESS	2007	SNR Shell	Mor	5-10?	-	[54]
Cassiopeia A	HEGRA	2001	SNR	Pos	3	$2.5 \pm 0.4$	[55]
Crab Nebula	Whipple	1989	PWN	Pos	100	$2.49 \pm 0.06$	[1, 56]
MSH 15-52	HESS	2005	PWN	Mor	15	$2.27 \pm 0.03$	[57]
Vela X	HESS	2006	PWN	Mor	75	$1.45 \pm 0.09^\dagger$	[58]
HESS J1825–137	HESS	2005	PWN	EDMor	12	$2.26 \pm 0.03^\dagger$	[40, 59, 60]
PSR J1420–6049	HESS	2006	PWN	Mor	7	$2.17 \pm 0.06$	[61]
The Rabbit	HESS	2006	PWN	Mor	6	$2.22 \pm 0.08$	[61]
G 0.9+0.1	HESS	2005	PWN	Pos	2	$2.40 \pm 0.11$	[62]

Table 2 lists those galactic VHE sources for which a multi-wavelength counterpart can be considered to be well established (note that such a classification is subjective and this is simply my personal view). There are three classes of such objects: supernova remnants, pulsar wind nebulae and binary systems:

*Shell-type Supernova Remnants* have long been considered as the likely acceleration site for the bulk of the galactic cosmic rays. As such they were prime targets for the first Cherenkov telescopes. The first (subsequently confirmed) SNRs to be detected at TeV energies were RX J1713.7–3946 [48] and Cassiopeia A [55], by the CANGAROO and HEGRA collaborations, respectively. The emission from RX J1713.7–3946 was resolved using H.E.S.S. as a shell with very similar morphology to that seen in non-thermal X-rays [49]. There are now three such resolved TeV shell SNR, shown in figure 4. These images demonstrate the existence of  $>$  TeV particles in the expanding shocks of

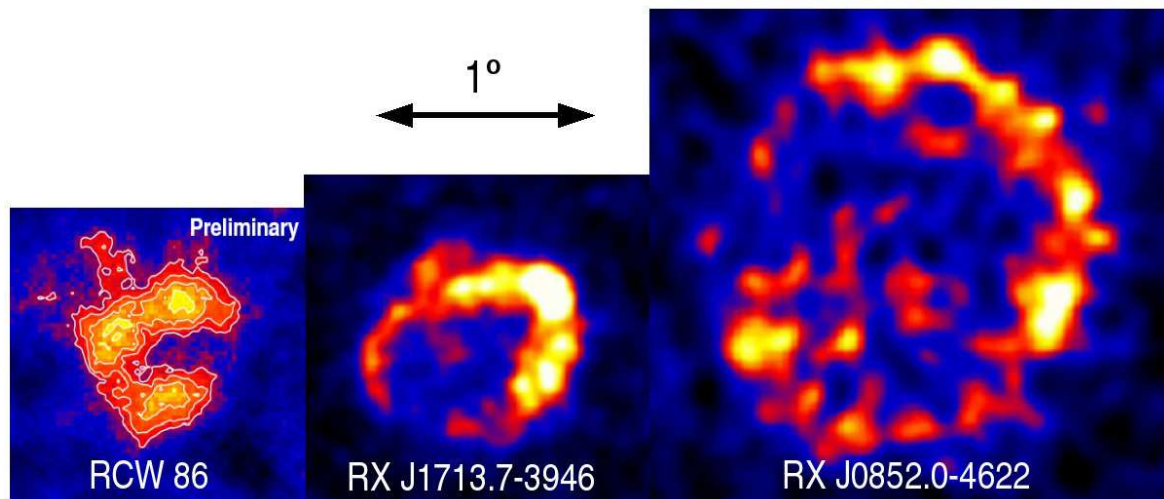


**Figure 4.** The shell-type TeV  $\gamma$ -ray supernova remnants: RCW 86 [54], RX J1713.7–3946 [63] and RX J0852.0–4622 (*Vela Junior*) [53]. All images are smoothed and were obtained using H.E.S.S.

these objects. However, the nature of the particles dominantly responsible for the TeV emission is still hotly debated.

Two basic scenarios have been widely discussed for the best measured object RX J1713.7–3946: 1) the  $\gamma$ -ray signal is inverse Compton emission from the same population of high energy electrons responsible for the synchrotron X-ray emission; 2) hadronic interactions of protons and nuclei lead to  $\gamma$ -ray emission via the decay of neutral pions. The first case is supported by correlation between X-ray and TeV emission, but implies a magnetic field close to  $10 \mu\text{G}$ , uncomfortably low in many models. The spectral shape of the  $\gamma$ -ray emission presents one way to break this ambiguity. Figure 5 compares the measured spectral energy distribution of RX J1713.7–3946 to expectations for three different scenarios. At present, hadronic models (see for example [64]) seem favoured for this object.

Another method to identify  $\gamma$ -ray emission as hadronic in origin is to establish a spatial correlation of the  $\gamma$ -ray emission with available target material. Indeed, such correlations seem to be present for the two (somewhat older:  $\sim 10^4$ – $10^5$  years cf  $\sim 1000$  years) SNRs W 28 and IC 443 in H.E.S.S. [67], MAGIC [68] and VERITAS [69] data, strongly suggesting that these objects are accelerating hadronic cosmic-rays. Such a correlation is also seen in the region of the Galactic Centre. However, in that particular case the acceleration site of the cosmic rays is not clear [70].

*Pulsar Wind Nebulae* (PWN) have now emerged as the largest population of identified TeV sources (see table 2). As the number of extended VHE  $\gamma$ -ray sources along the Galactic Plane has increased, the likelihood of chance associations with pulsars is now far from negligible. A systematic search for coincidences between sources detected in the H.E.S.S. galactic plane survey and radio pulsars has recently been performed by the

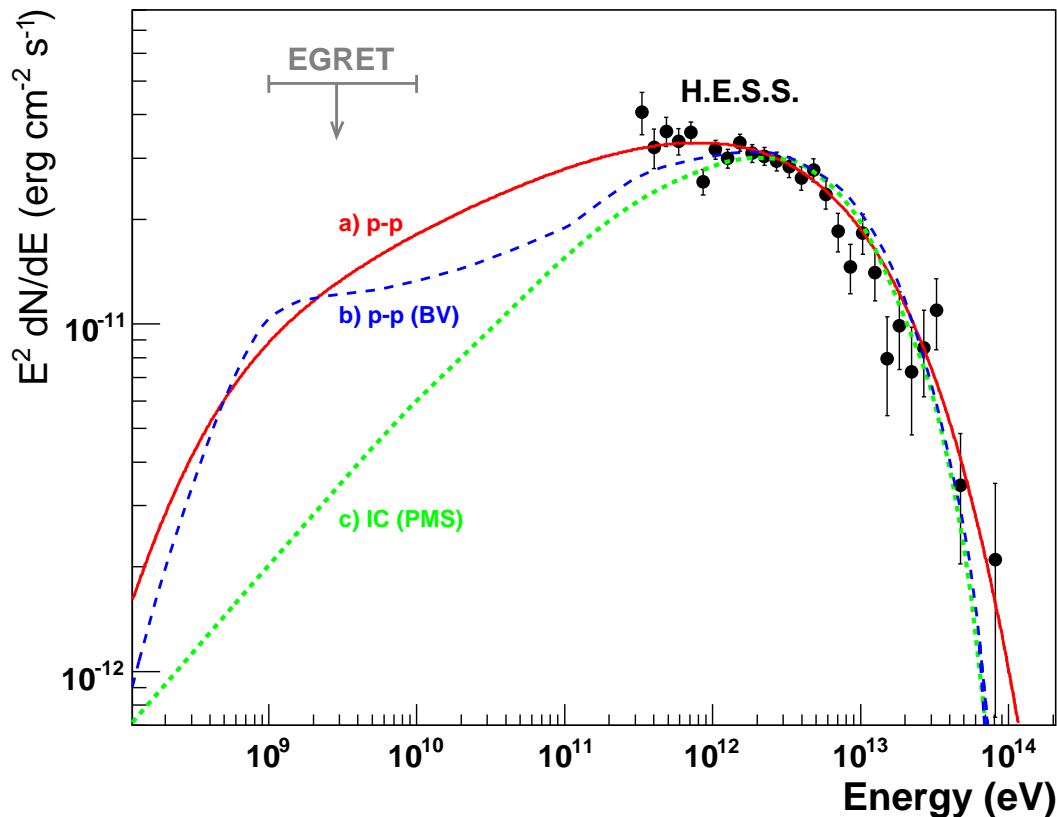


**Figure 5.** The spectral energy distribution of RX J1713.7–3946 in the  $\gamma$ -ray range. The TeV data points are taken from [63], model curves are given for three scenarios: (a) a fit of the function  $dN/dE \propto E^{-\Gamma} \exp -\sqrt{E/E_0}$ , the approximate form expected for interacting protons with a energy distribution following a power-law with exponential cut-off, see [63] and [65]. (b) hadronic emission as calculated by [64], and (c) inverse Compton emission as calculated by [66].

H.E.S.S. collaboration [71]. A clear excess of  $\gamma$ -ray nebulae in positional coincidence with high spin-down luminosity pulsars (those with  $\dot{E}/d^2$  above  $\sim 10^{35} \text{ erg s}^{-1} \text{ kpc}^{-2}$ ) is found, in comparison to expectations for chance coincidences. The implied efficiency in the conversion of spin-down power, via ultra-relativistic winds, into TeV  $\gamma$ -ray production is around 1%. A key recent result in this area, is that of energy-dependant morphology in HESS J1825–137 [60]. New H.E.S.S. data show that the  $\gamma$ -ray emission ‘shrinks’ at high energies: towards the pulsar PSR B1823–13. Such behaviour has been seen before in X-ray synchrotron emission and has been interpreted as evidence for the energy-losses of  $> \text{TeV}$  electrons. The discovery of this effect in  $\gamma$ -rays provides us with a potentially powerful new tool with which to investigate high energy particles within these objects.

The remaining well established class of galactic TeV sources is that of *binary systems* of a compact object and a massive star. Three such systems have now been firmly identified (see table 2). These objects appear to belong to one of two classes: microquasars or binary PWN. Whilst the 3.4 year period system of PSR B1259–63 and the Be-star SS2883 certainly belongs to the later class, in the two remaining well

established systems, LS 5039 and LSI+61 303 the acceleration site is not yet clear. In the binary pulsar scenario the energy source is the spin-down of the neutron star, in the microquasar scenario accretion is the power-source and the particle acceleration occurs in relativistic jets produced close to the compact object (black hole or neutron star). The best  $\gamma$ -ray microquasar candidate so far is perhaps Cyg X-1, in which the compact object is certainly a black hole. However, the evidence for TeV emission from this object has not yet reached the level where a robust detection claim can be made [72]. See [73] for a recent review of this topic.

Beyond these established TeV source classes there are indications of an emerging class of sources associated with *clusters of massive young stars*. The colliding winds of massive stars are thought to result in strong shocks capable of accelerating particles up to TeV energies (see for example [74] and [75]) and particularly, the collective effect of such winds could be detectable in  $\gamma$ -rays. The recently discovered  $\gamma$ -ray source HESS J1023–575 [76] is coincident with the massive stellar cluster Westerlund 2: the second most massive young cluster in our galaxy. Whilst this association may be coincidental, the colliding winds of stars in this cluster can certainly provide the energy required to produce the  $\gamma$ -ray emission and acceleration in such objects seems plausible.

#### 4.2. Extragalactic Sources

Extragalactic objects so far face none of the identification problems of galactic sources, to date all are point-like and no serendipitous discoveries have been made. Indeed, so far all extragalactic  $\gamma$ -ray sources appear to be Active Galactic Nuclei (AGN). AGN are believed to host actively accreting  $> 10^6$  solar mass black holes which drive powerful relativistic jets into their environments. The *blazar* subclass of AGN is characterised rapid variability and broad-band non-thermal emission. These objects are thought to represent AGN with jets aligned very closely ( $< 10^\circ$ ) with the line of sight to the observer, resulting in fluxes enhanced through beaming effects.

Table 3 lists the known TeV emitting AGN in order of redshift. This table shows that more distant objects ( $z > 0.13$ ) have been discovered only in the past two years. This is a consequence of the attenuation of TeV photons via pair-production on the extragalactic background light (EBL) (see for example [77]). This absorption provides an effective horizon to the universe which expands rapidly at low energies. Sensitive instruments with low energy thresholds are therefore required to detect distant objects. The distance corresponding at an optical depth of one is approximately  $z = 0.1$  at 1 TeV. Only relatively recently have experiments with substantial sensitivity in the 0.05–1 TeV range existed, leading to a rapid expansion in the number of  $z > 0.1$  TeV blazars. Table 3 reveals some evidence for the expected softening of spectra at larger redshift, but the intrinsic spread in blazar spectral properties is clearly very large.

The distortion of  $\gamma$ -ray spectra by extragalactic attenuation, though problematic for TeV studies of distant objects, can be used to advantage in deriving limits on the wavelength dependent density of the EBL. Under the assumption that the intrinsic

**Table 3.** The known very high energy  $\gamma$ -ray emitting AGN. Only statistical errors are given on the photon index. The final column gives the reference to the discovery publication and also the reference for the photon index, where different.

Object	Discovered	Year	$z$	Class	Photon Index	Ref.
M 87	HEGRA	2003	0.004	LINER	$2.22 \pm 0.15$	[83, 84]
Mrk 421	Whipple	1992	0.031	HBL	$2.56 \pm 0.07$	[85, 86]
Mrk 501	Whipple	1996	0.034	HBL	$2.47 \pm 0.07$	[87, 88]
1ES 2344+514	Whipple	1998	0.044	HBL	$2.54 \pm 0.17$	[89, 90]
Mrk 180	MAGIC	2006	0.046	HBL	$3.3 \pm 0.7$	[91]
1ES 1959+650	TA	2002	0.047	HBL	$2.83 \pm 0.14$	[92, 93]
BL Lac	MAGIC	2006	0.069	LBL	$3.6 \pm 0.5$	[94]
PKS 0548-322	HESS	2006	0.069	HBL	-	[95]
PKS 2005-489	HESS	2005	0.071	HBL	$4.0 \pm 0.4$	[96]
PKS 2155-304	Durham	1999	0.116	HBL	$3.32 \pm 0.06$	[97, 98]
H 1426+428	Whipple	2002	0.129	HBL	$3.50 \pm 0.35$	[99, 100]
1ES 0229+200	HESS	2007	0.140	HBL	$2.50 \pm 0.19$	[79]
H 2356-309	HESS	2005	0.165	HBL	$3.06 \pm 0.21$	[78]
1ES 1218+304	MAGIC	2005	0.182	HBL	$3.0 \pm 0.4$	[101]
1ES 1101-232	HESS	2005	0.186	HBL	$2.88 \pm 0.17$	[78]
1ES 0347-121	HESS	2007	0.188	HBL	$3.10 \pm 0.23$	[80]
1ES 1011+496	MAGIC	2007	0.212	HBL	$4.0 \pm 0.5$	[102]
PG 1553+113	HESS	2005	$> 0.25$	HBL	$4.0 \pm 0.6$	[103]
3C 279	MAGIC	2007	0.536	FSRQ	-	[82]

spectrum of these objects has a photon index not less than 1.5 (that expected for inverse Compton radiation of an  $E^{-2}$  electron spectrum radiating in the Thompson limit), limits on the near mid- and near infra-red EBL have been calculated that approach the lower limits from galaxy counts at these wavelengths, effectively resolving the EBL density at these wavelengths [78, 79, 80, 81]. The spectrum of the EBL provides important constraints on the star formation history of the universe. For example, the TeV limits in the near infra-red range can be used to place limits on the contribution of the first generation of stars [78]. The recent detection of the  $z = 0.536$  flat spectrum radio quasar 3C 279 by the MAGIC collaboration represents a major step forward in distance, and promises to be very important for constraining the EBL at shorter wavelengths [82].

The activity of the TeV blazar PKS 2155–304 observed using H.E.S.S. in July 2006 was the most dramatic seen so far from any object in VHE  $\gamma$ -rays [104]. Figure 6 shows the light curve of the night with the highest flux, during which the emission reached two orders of magnitude higher fluxes than those typically seen from this object. Variability is clearly visible on timescales of a few minutes in figure 6 and the best measured individual flare is the first of the night with a best fit rise-time of  $173 \pm 23$  seconds. Such rapid variability suggests an extremely large Doppler factor ( $\sim 100$ ), approaching that seen for Gamma-ray Bursts and extremely challenging for models. Activity from Mrk 501 at a somewhat lower level was detected using MAGIC one year earlier [105], and is interesting due to the evidence for *time-lags* between activity in different VHE energy bands. The absence of lags has been used in the past to constrain any possible energy

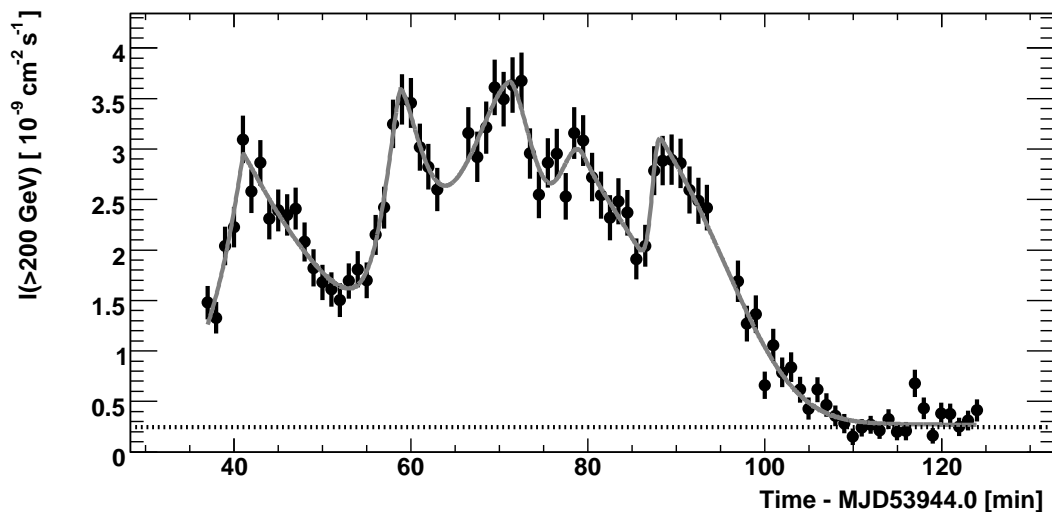


**Figure 6.**  $\gamma$ -ray light curve, in one minute bins, of the spectacular flare from PKS 2155–304 detected using H.E.S.S. in July 2006. Reproduced from [104].

dependence of the speed of light (due for example to quantum gravity effects) [106]. Whilst it is quite plausible that the lags are intrinsic to the source due to the different acceleration and energy loss timescales of particles of different energies, the MAGIC result may be the first hint for new physics [107]. The H.S.S.S. data from PKS 2155–304 should allow this hypothesis to be tested in the near future.

The nearby radio galaxy M 87 has a jet inclined at  $\sim 30^\circ$  to the line of sight and is hence the only non-blazar extragalactic TeV source. Given the reduced beaming effects in such a system, and the mass of the black hole ( $\approx 3 \times 10^9$  solar masses), the two day timescale variability discovered using H.E.S.S. [84] is particularly surprising. Causality arguments have been used to derive a limit of  $5\delta R_s$  on the size of the emission region, where  $\delta$  is the Doppler factor of the source and  $R_s$  is the Schwarzschild radius of the supermassive black hole. Figure 7 shows the light-curve of M 87 on long (year) and short (day) timescales including data from several VHE instruments. The most recent data shown are the  $5.1\sigma$  detection of this source using VERITAS earlier this year [108].

## 5. Summary

Cherenkov telescope arrays have proved themselves to be the most effective way to pursue (photon) astronomy at the highest energies. Of the 71 currently known TeV  $\gamma$ -ray sources, 68 were discovered using the imaging Cherenkov technique. Whilst the alternative approach, based on shower particle detection at ground level, is clearly complementary due to the much wider field of view and duty cycle achievable, Cherenkov instruments are likely to remain the work-horse of the field for some time. The sensitivity and precision obtain with this technique are unrivalled in the high energy ( $> \text{MeV}$ ) domain. An order of magnitude improvement in sensitivity should be achievable with

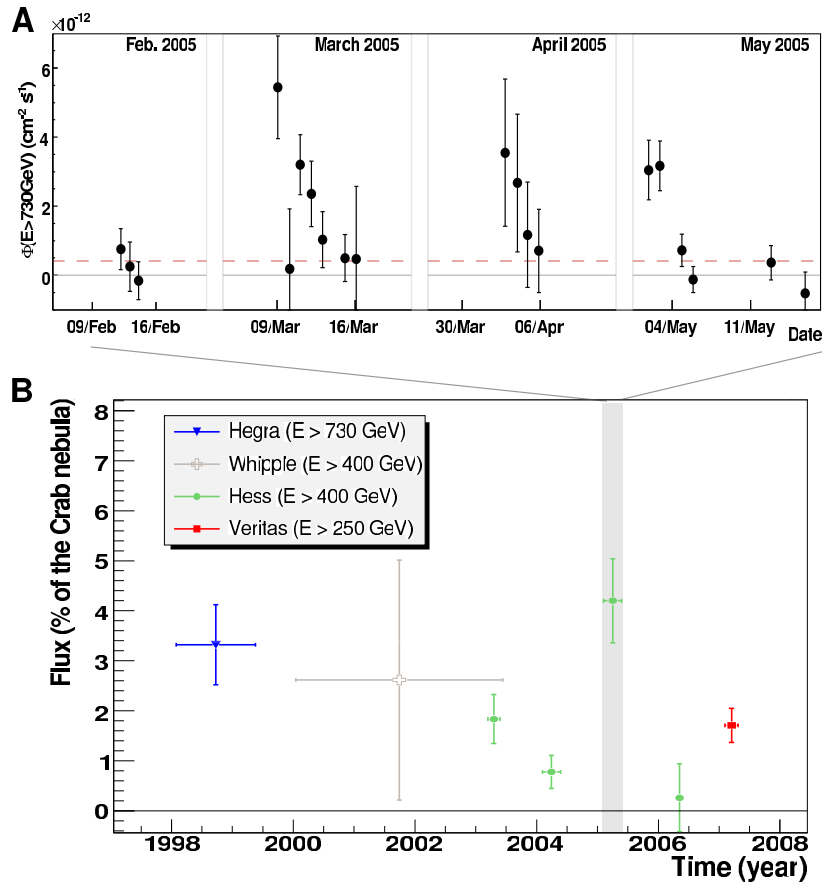


**Figure 7.** Long and short-term variability in the TeV emission of M 87. A) Short-term variability seen in the light-curve of M 87 using H.E.S.S. in 2005, reproduced from [84] and B) Long-term variability as seen using HEGRA, Whipple, H.E.S.S. and VERITAS, reproduced from [108].

next generation instruments such as CTA and AGIS, which are discussed elsewhere in this issue.

The most important recent scientific highlights produced using this technique are perhaps the ongoing survey of our galaxy with H.E.S.S., which has resulted in the discovery of a large fraction of the known TeV sources, and the recent detections of distant ( $z \gg 0.1$ ) AGN using H.E.S.S. and MAGIC, marking very significant expansion of volume of the universe accessible to ground-based  $\gamma$ -ray instruments. The potential for new discoveries seems to be very large, with several source classes, for example Clusters of Galaxies and Starbursts, predicted to emit at flux levels very close to current sensitivity limits. VHE  $\gamma$ -ray astronomy using Cherenkov Telescope arrays can now be regarded as a well established astronomical discipline — with a very bright future.

## Acknowledgments

I would like to thank all authors who agreed to provide plots and J. Skilton for her careful reading of the manuscript.

## References

- [1] T. C. Weekes et al. 1989 *ApJ* 342, 379
- [2] W. Hofmann 2006 *ArXiv e-prints* astro-ph/0603076
- [3] J. Rico, E de Ona-Wilhelmi, J. Cortina, and E. Lorenz. 2007 *ArXiv e-prints* 0709.2283
- [4] K. Kosack et al. 2004 *ApJ* 608, L97
- [5] F. Aharonian et al. 2005 *A&A* 437, 95
- [6] F. A. Aharonian, A. K. Konopelko, H. J. Völk, and H. Quintana. 2001 *Astroparticle Physics* 15, 335
- [7] I. de La Calle Pérez and S. D. Biller. 2006 *Astroparticle Physics* 26, 69
- [8] A. M. Hillas 1985 *19th International Cosmic Ray Conference, La Jolla, USA*, 3, 445
- [9] A. M. Hillas 1996 *Space Science Reviews* 75, 17
- [10] F. Piron et al. 2001 *A&A* 374, 895
- [11] M. de Naurois 2006 *ArXiv e-prints* astro-ph/0607247
- [12] M. Lemoine-Goumard, B. Degrange, and M. Tluczykont 2006 *Astroparticle Physics* 25, 195
- [13] D. Berge, S. Funk, and J. Hinton 2007 *A&A* 466, 1219
- [14] A. Daum et al. 1997 *Astroparticle Physics* 8, 1
- [15] S. Funk et al. 2004 *Astroparticle Physics* 22, 285
- [16] R. W. Lessard et al. 2001 *Astroparticle Physics* 15, 1
- [17] A. Konopelko et al. 1999 *Astroparticle Physics* 10, 275
- [18] R. Mirzoyan, D. Sobczynska, E. Lorenz, and M. Teshima 2006 *Astroparticle Physics* 25, 342
- [19] V. R. Chitnis and P. N. Bhat 2001 *Astroparticle Physics* 15, 29
- [20] D. Tescaro et al. 2007 *ArXiv e-prints* 0709.1410
- [21] J. A. Hinton 2004 *New Astronomy Review* 48, 331
- [22] K. Bernlöhr et al. 2003 *Astroparticle Physics* 20, 111
- [23] P. Vincent et al 2005 *29th International Cosmic Ray Conference, Pune, India* 5, 163
- [24] J. Cortina 2005 *Ap&SS* 297, 245
- [25] J. Cortina et al. 2005 *29th International Cosmic Ray Conference, Pune, India* 5, 359
- [26] C. C. Hsu et al. 2007 *ArXiv e-prints* 0709.2474,
- [27] J. Holder et al. 2006 *Astroparticle Physics* 25, 391
- [28] J. Holder et al. 2006 *ArXiv e-prints* astro-ph/0611598
- [29] G. Maier et al. 2007 *ArXiv e-prints* 0709.3654,
- [30] H. Kubo et al. 2004 *New Astronomy Review* 48, 323
- [31] S. Ebisuzaki et al. 1991 *22nd International Cosmic Ray Conference, Dublin, Ireland* 2, 607
- [32] T. Yoshikoshi et al. 1999 *Astroparticle Physics* 11, 267
- [33] M. Mori et al. 2007 *30th International Cosmic Ray Conference, Merida, Mexico*
- [34] R. Koul et al. 2007 *Nuc. Instr. and Meth. in Phys. Research A* 578, 548
- [35] D. Bose et al. 2007 *Ap&SS* 309, 111
- [36] J. Bussons Gordo 2004 *New Astronomy Reviews* 48, 351
- [37] D. A. Williams et al. 2004 *New Astronomy Reviews* 48, 359
- [38] T. Tümer et al. 1999 *Astroparticle Physics* 11, 271
- [39] F. Arqueros et al. 2002 *Astroparticle Physics* 17, 293
- [40] F. Aharonian et al. 2005 *Science* 307, 1938
- [41] F. Aharonian et al. 2006 *ApJ* 636, 777
- [42] S. Hoppe et al. 2007 *ArXiv e-prints* 0710.3528



- [43] F. Aharonian et al. 2005 *A&A* 442, 1
- [44] F. Aharonian et al. 2005 *Science* 309, 746
- [45] F. Aharonian et al. 2006 *A&A* 460, 743
- [46] J. Albert et al. 2006 *Science* 312, 1771
- [47] V. A. Acciari et al. 2008 *ArXiv e-prints* 0802.2363,
- [48] H. Muraishi et al. 2000 *A&A* 354, L57
- [49] F. A. Aharonian et al. 2004 *Nature* 432, 75
- [50] F. Aharonian et al. 2005 *A&A* 449, 223
- [51] H. Katagiri et al. 2005 *ApJ* 619, L163
- [52] F. Aharonian et al. 2005 *A&A* 437, L7
- [53] F. Aharonian et al. 2007 *ApJ* 661, 236
- [54] S. Hoppe et al. 2007 *30th International Cosmic Ray Conference, Merida, Mexico*
- [55] F. Aharonian et al. 2001 *A&A* 370, 112
- [56] A. M. Hillas et al. 1998 *ApJ* 503, 744
- [57] F. Aharonian et al. 2005 *A&A* 435, L17
- [58] F. Aharonian et al. 2006 *A&A* 448, L43
- [59] F. A. Aharonian et al. 2005 *A&A* 442, L25
- [60] F. Aharonian et al. 2006 *A&A* 460, 365
- [61] F. Aharonian et al. 2006 *A&A* 456, 245
- [62] F. Aharonian et al. 2005 *A&A* 432, L25
- [63] F. Aharonian et al. 2007 *A&A* 464, 235
- [64] E. G. Berezhko and H. J. Völk 2006 *A&A* 451, 981
- [65] S. R. Kelner, F. A. Aharonian, and V. V. Bugayov 2006 *Phys. Rev. D* 74, 034018
- [66] T. A. Porter, I. V. Moskalenko, and A. W. Strong 2006 *ApJ* 648, L29
- [67] G. Rowell et al. 2007 *ArXiv e-prints* 0710.2017
- [68] J. Albert et al. 2007 *ApJ* 664, L87
- [69] T. B. Humensky et al. 2007 *30th International Cosmic Ray Conference, Merida, Mexico*
- [70] F. Aharonian et al. 2007 *Nature* 439, 695
- [71] S. Carrigan et al. 2007 *ArXiv e-prints* 0709.4094
- [72] J. Albert et al. 2007 *ApJ* 665, L51
- [73] I. F. Mirabel 2006 *Science* 312, 1759
- [74] E. Domingo-Santamaría and D. F. Torres 2006 *A&A* 448, 613
- [75] J. M. Pittard and S. M. Dougherty 2006 *MNRAS* 372, 801
- [76] F. Aharonian et al. 2007 *A&A* 467, 1075
- [77] G. G. Fazio and F. W. Stecker 1970 *Nature* 226, 135
- [78] F. Aharonian et al. 2006 *Nature* 440, 1018
- [79] F. Aharonian et al. 2007 *A&A* 475, L9
- [80] F. Aharonian et al. 2007 *A&A* 473, L25
- [81] D. Mazin and M. Raue 2007 *A&A* 471, 439
- [82] M. Teshima et al. 2007 *ArXiv e-prints* 0709.1475,
- [83] F. Aharonian et al. 2003 *A&A* 403, L1
- [84] F. Aharonian et al. 2006 *Science* 314, 1424
- [85] M. Punch et al. 1992 *Nature* 358, 477
- [86] J. A. Zweerink et al. 1997 *ApJ* 490, L141
- [87] J. Quinn et al. 1996 *ApJ* 456, L83
- [88] F. Aharonian et al. 1997 *A&A* 327, L5
- [89] M. Catanese et al. 1998 *ApJ* 501, 616
- [90] M. Schroedter et al. 2005 *ApJ* 634, 947
- [91] J. Albert et al. 2006 *ApJ* 648, L105
- [92] T. Nishiyama et al. 1999 *26th International Cosmic Ray Conference, Salt Lake City, USA* 3, 370
- [93] F. Aharonian et al. 2003 *A&A* 406, L9

- [94] J. Albert et al. 2007 *ApJ* 666, L17
- [95] G. Superina, et al. 2007 *30th International Cosmic Ray Conference, Merida, Mexico*
- [96] F. Aharonian et al. 2005 *A&A* 436, L17
- [97] P. M. Chadwick et al. 1999 *ApJ* 513, 161
- [98] F. Aharonian et al. 2005 *A&A* 430, 865
- [99] D. Horan et al. 2002 *ApJ* 571, 753
- [100] D. Petry et al. 2002 *ApJ* 580, 104
- [101] J. Albert et al. 2006 *ApJ* 642, L119
- [102] J. Albert et al. 2007 *ApJ* 667, L21
- [103] F. Aharonian et al. 2006 *A&A* 448, L19
- [104] F. Aharonian et al. 2007 *ApJ* 664, L71
- [105] J. Albert et al. 2007 *ApJ* 669, 862
- [106] S. D. Biller et al. 1999 *Physical Review Letters* 83, 2108
- [107] J. Albert et al. 2007 *ArXiv e-prints* 0708.2889
- [108] P. Colin et al. 2007 *30th International Cosmic Ray Conference, Merida, Mexico*